Optica Applicata, Vol. XLII, No. 3, 2012
DOI: 10.5277/oa120305

Focus shaping of Bessel–Gauss beam with radial varying polarization

XIUMIN GAO[1, 2*], RUI FU[1], HAIBIN SHEN[2], XIANGMEI DONG[3], TAO GENG[3], SONGLIN ZHUANG[3]

[1]Electronics and Information College, Hangzhou Dianzi University, Hangzhou 310018, China

[2]China Jiliang University, Hangzhou 310018, China

[3]University of Shanghai for Science and Technology, Shanghai 200093, China

[*]Corresponding author: xiumin_gao@yahoo.com.cn

Focusing properties of Bessel–Gauss beam with radial varying polarization are investigated based on vector diffraction theory in this article. The polarization angle formed by polarization direction and radial coordinate is the function of the radial distance in pupil plane, and one polarization parameter indicates the speed of change of polarization angle. It was found that the intensity distribution in focal region can be altered considerably by the beam parameter and polarization parameter. For a small beam parameter, the focal spot broadens transversely, distorts into ring focus, and then evolves back into focal spot on increasing polarization parameter. When beam parameter gets higher, focal pattern becomes complicated and the focus evolution principle with increasing beam parameter also changes significantly. Some novel focal patterns may appear, including multiple intensity rings, dark hollow focus, cylindrical crust focus.

Keywords: focusing properties, Bessel–Gauss beam, vector diffraction theory.

1. Introduction

Intensity distribution in focal region plays an important role in many optical systems [1–6]. For instance, in optical trapping system, it is usually deemed that the forces exerted on the particle in light field are twofold, one is the optical gradient force, which plays a crucial role in constructing optical trap and its intensity is proportional to the optical intensity gradient; the other is scattering force, which usually has complex forms because this kind of force is related to the properties of the trapped particles, and whose intensity is proportional to the optical intensity [7]. Therefore, tunable optical intensity distribution in focal region means that the controllable optical trap may occur. Dark focal spot refers to those focuses whose optical intensity is weaker than that around it and is stable optical trap for those particles whose refractive index is smaller than that of surrounding media, and this condition is very common,

especially in life science [8]. Dark focal spot may be stable trap for those particles whose refractive index is smaller than that of surrounding media. Therefore, construction of dark focal spot is very important and attracts interest of many researchers [9–11].

On the other hand, laser beams with cylindrical symmetry in polarization have recently attracted attention of many researchers for their interesting properties and applications [12–17]. YOUNGWORTH and BROWN calculated cylindrical-vector fields [14] and showed that, in the particular case of a tightly focused radially polarized beam, the polarization reveals large inhomogeneities in the focal region, while the azimuthally polarized beam is purely transverse. Therefore, the polarization distribution affects focus shape very considerably. In addition, it is known that Bessel–Gauss (BG) beams provide valid solutions to Helmholtz equation, and have attracted a lot of attention [18–25] for their non-diffracting property. BG beams represent a class of so-called diffraction free solutions to the Helmholtz equation, and have been studied extensively since 1980s [18], and these beams are easily generated by illuminating an axicon with a Gaussian beam [25]. Recently, BG beam with radial varying polarization was introduced, and its application in optical tweezers was also discussed briefly [26]. In this article, focusing properties of BG beam with radial varying polarization are investigated in detail. In Section 2, the principle of the focusing system is given. Simulation results and discussion are shown in Section 3. Conclusions are given in Section 4.

2. Focusing BG beam with radial varying polarization

The incident beam we investigated here is BG beam with radial varying polarization, and using the same analysis method as that in references [12–14], the electric field in focal region can be written in the form of [12–14],

$$\mathbf{E}(r,\varphi,z) = E_r\mathbf{e_r} + E_\varphi\mathbf{e}_\varphi + E_z\mathbf{e_z} \tag{1}$$

where $\mathbf{e_r}$, $\mathbf{e}_\varphi$, and $\mathbf{e_z}$ are the unit vectors in the radial, azimuthal, and propagating directions, respectively; E_r, E_φ, and E_z are amplitudes of the three orthogonal components and can be expressed as

$$E_r(r,z) = A\cos(\phi)\int_0^\alpha \cos^{1/2}(\theta)P(\theta)\sin(2\theta)\,J_1\Big(kr\sin(\theta)\Big)\exp\Big[ikz\cos(\theta)\Big]\mathrm{d}\theta \tag{2}$$

$$E_\varphi(r,z) = 2A\cos(\phi)\int_0^\alpha \cos^{1/2}(\theta)P(\theta)\sin(2\theta)\,J_1\Big(kr\sin(\theta)\Big)\exp\Big[ikz\cos(\theta)\Big]\mathrm{d}\theta \tag{3}$$

$$E_z(r, z) = 2iA\cos(\phi)\int_0^{\alpha}\cos^{1/2}(\theta)P(\theta)\sin^2(\theta)\,J_0\left(kr\sin(\theta)\right)\exp\left[ikz\cos(\theta)\right]\mathrm{d}\theta \tag{4}$$

where r and z are the radial and propagating coordinates of observation point in focal region, respectively; k is the wave number, $P(\theta)$ is the pupil apodization function [27],

$$P(\theta) = J_1\left(\frac{2\beta_1\sin(\theta)}{\mathrm{NA}}\right)\exp\left[-\left(\frac{\beta_2\sin(\theta)}{\mathrm{NA}}\right)^2\right] \tag{5}$$

and α = asin(NA), which practically indicates the radius corresponding to each section zone of the cylindrical vector beam. It should be noted that the parameters β_1 and β_2 are defined as ratios of pupil diameter to the beam radius [27]. Parameters β_1 and β_2 indicate the effect of the Bessel and Gaussian function in Eq. (5) on the am-plitude distribution, respectively; ϕ is the polarization rotation angle from radial direction, in this article, ϕ is the function of convergence angle θ, and is written as [26],

$$\phi = C\frac{\sin(\theta)}{\sin(\alpha)}\pi \tag{6}$$

where C is polarization parameter that indicates the speed of change of polarization angle. Therefore, the electric field can be rewritten as,

$$\mathbf{E}(r, \varphi, z) = X + Y + Z \tag{7}$$

where

$$X = A\int_0^{\alpha}\cos^{1/2}(\theta)\sin(2\theta)\cos\left[C\frac{\sin(\theta)}{\sin(\alpha)}\pi\right]\times$$

$$\times J_1\left(\frac{2\beta_1\sin(\theta)}{\mathrm{NA}}\right)\exp\left[-\left(\frac{\beta_2\sin(\theta)}{\mathrm{NA}}\right)^2\right]J_1\left(kr\sin(\theta)\right)\exp\left[ikz\cos(\theta)\right]\mathrm{d}\theta\,\mathbf{e_r}$$

$$Y = 2iA\int_0^{\alpha}\cos^{1/2}(\theta)\sin^2(\theta)\cos\left[C\frac{\sin(\theta)}{\sin(\alpha)}\pi\right]\times$$

$$\times J_1\left(\frac{2\beta_1\sin(\theta)}{\mathrm{NA}}\right)\exp\left[-\left(\frac{\beta_2\sin(\theta)}{\mathrm{NA}}\right)^2\right]J_0\left(kr\sin(\theta)\right)\exp\left[ikz\cos(\theta)\right]\mathrm{d}\theta\,\mathbf{e_z}$$

$$Z = 2A\int_0^{\alpha}\cos^{1/2}(\theta)\sin(\theta)\sin\left[C\frac{\sin(\theta)}{\sin(\alpha)}\pi\right]\times$$

$$\times J_1\left(\frac{2\beta_1\sin(\theta)}{\mathrm{NA}}\right)\exp\left[-\left(\frac{\beta_2\sin(\theta)}{\mathrm{NA}}\right)^2\right]J_1\left(kr\sin(\theta)\right)\exp\left[ikz\cos(\theta)\right]\mathrm{d}\theta\,\mathbf{e}_{\varphi}$$

The optical intensity in focal region is proportional to the modulus square of Eq. (7). Based on this equation, the focus shape can be investigated numerically.

3. Numerical results and discussion

Without losing generality and validity, it is supposed that A unit one. It should be noted that the distance unit in all the figures is the wavelength of incident beam in vacuum. Firstly, the intensity distributions in focal region under condition of NA = 0.95, $\beta_2 = 1$, $\beta_1 = 0.5$, and different C were calculated and shown in Fig. 1. The effect of parameters β_1 and β_2 on focal shape will be investigated, with $\beta_2 = 1$ and $\beta_1 = 0.5$ being only chosen as one case, then their values will be changed to get insight into their effect. We can see from this figure that there is only one intensity peak for small C. On increasing C, the focal spot extends in transverse direction, and then one intensity spot changes into one ring shape, namely, one ring focus comes into being. When the parameter C increases continuously, the radius of the ring focus increases firstly, and then decreases remarkably. For higher C, the ring focus shrinks back into one

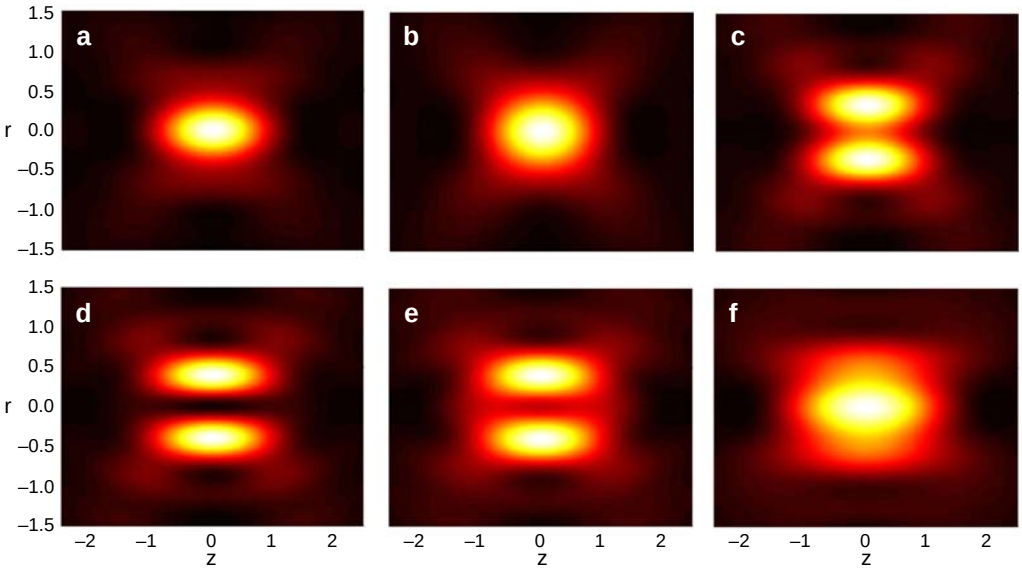

Fig. 1. Intensity distributions in focal region for NA = 0.95, $\beta_2 = 1$, $\beta_1 = 0.5$; $C = 0.0$ (**a**), $C = 0.2$ (**b**), $C = 0.4$ (**c**), $C = 0.6$ (**d**), $C = 0.8$ (**e**), and $C = 1.0$ (**f**).

intensity peak, namely, there is again one focus spot though it is a distorted spheroid, as shown in Fig. 1**f**.

In order to show the intensity more clearly, the corresponding transverse intensity distribution curves are also given in Fig. 2. If one focal spot is regarded as one special case of the ring focus, namely, the radius of ring focus is zero, we can investigate the dependence of the radius on the increasing *C*. Figure 3 illustrates the dependence of the radius of ring focus on increasing *C*. The radius is zero for small *C*. And on increasing *C*, the radius increases firstly, and then maintains higher value for certain *C* range. When *C* increases continuously, the radius decreases sharply, and finally falls to zero, as shown in Fig. 3.

Now, the parameter β_1 is chosen as 1.5, the intensity distributions in focal region for NA = 0.95, β_2 = 1, β_1 = 1.5, and different *C* are calculated and shown in Fig. 4. It can be seen from this figure that there is only one intensity peak for small *C*. On increasing *C*, the center focal spot extends transversely, and focus changes into one ring focal shape. When *C* increases continuously, the radius of the ring focus

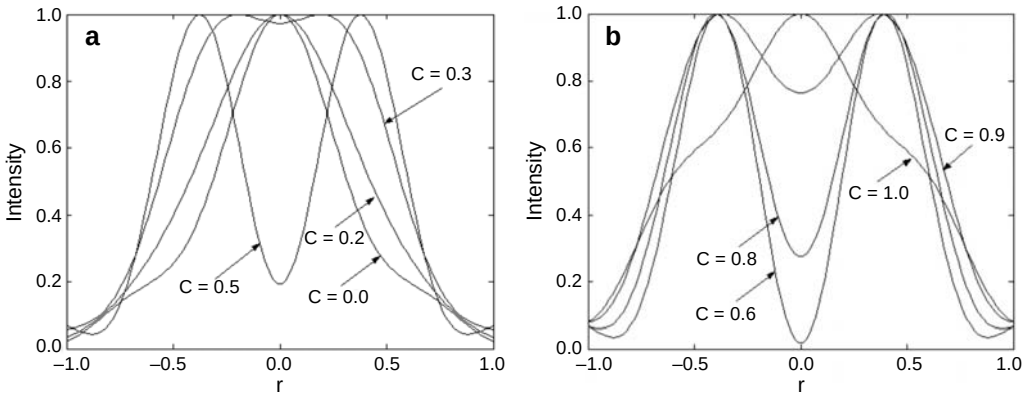

Fig. 2. Transverse intensity distributions for NA = 0.95, β_2 = 1, β_1 = 0.5. Smaller *C* (**a**) and bigger *C* (**b**).

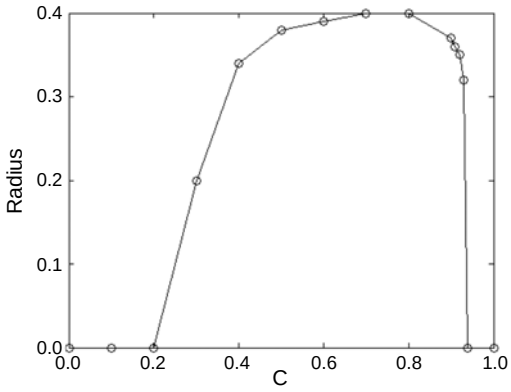

Fig. 3. Dependence of the radius of ring focus on increasing *C*.

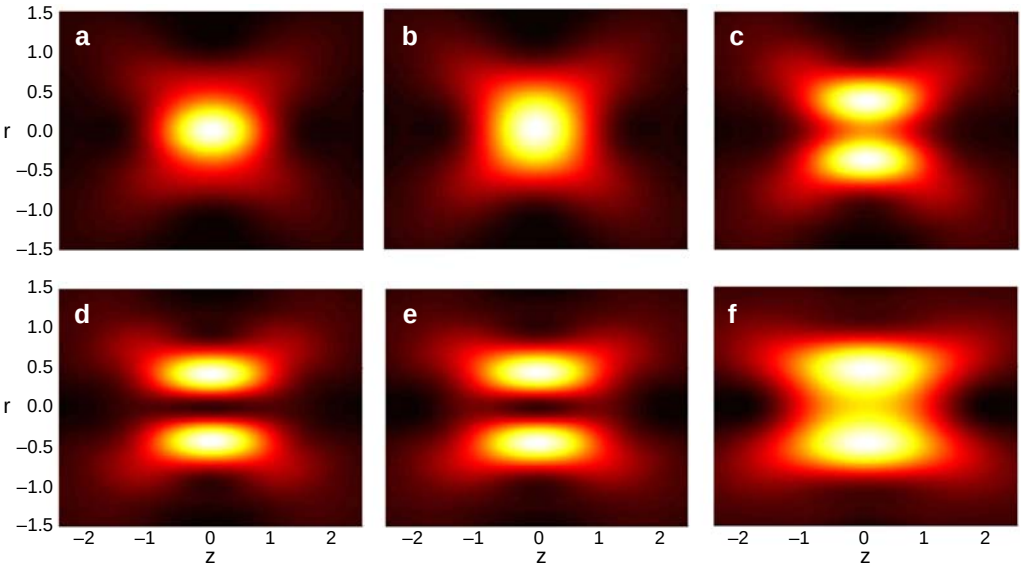

Fig. 4. Intensity distributions in focal region for NA = 0.95, $\beta_2 = 1$, $\beta_1 = 1.5$, and $C = 0.0$ (**a**), $C = 0.2$ (**b**), $C = 0.4$ (**c**), $C = 0.6$ (**d**), $C = 0.8$ (**e**), and $C = 1.0$ (**f**).

increases, and then decreases on increasing C. Though the whole focal pattern evolution principle shown in Fig. 4 is very similar to that under condition of $\beta_1 = 0.5$, by comparing Fig. 4 with Fig. 1, we can see that the focal spot extends transversely under condition of higher β_1. Therefore, β_1 affects focal pattern considerably.

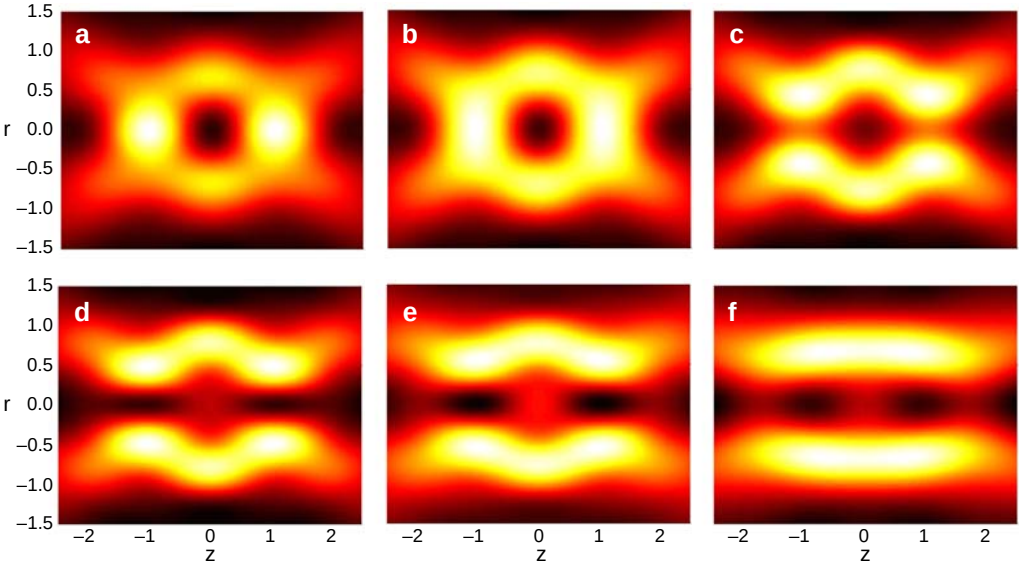

Fig. 5. Intensity distributions in focal region for NA = 0.95, $\beta_2 = 1$, $\beta_1 = 2.5$, and $C = 0.0$ (**a**), $C = 0.2$ (**b**), $C = 0.4$ (**c**), $C = 0.6$ (**d**), $C = 0.8$ (**e**), and $C = 1.0$ (**f**).

When the parameter β_1 increases to 2.5, the focal pattern changes very remarkably, as shown in Fig. 5. We can see from this figure that there occurs one quasi-spherical crust intensity distribution for small C. And its two intensity maximum peaks are located on optical axis. Dark focal spot comes into being in this case, which may be used to construct stable trap for those particles whose refractive index is smaller than that of surrounding media. On increasing C, the two intensity peaks extend transversely, as shown in Fig. 5**b**. And when the parameter C increases continuously, these two peaks change into two ring intensity distributions, at the same time, the intensity distribution in geometrical focal plane also becomes local maximum ring shape. These three overlapping ring intensity distributions lead to the whole focal pattern evolution from the quasi-spherical crust focal pattern to the cylindrical crust focal pattern, and the center dark focal spot also disappears on increasing C. Finally, the three intensity rings combine into one smooth cylindrical crust intensity distribution, as shown in Fig. 5**f**. From the above focal pattern evolution it can be seen that the parameter β_1 affects focal pattern considerably, and some novel focal patterns occur, which may be used in optical tweezers technology.

For the parameter β_1 increasing to 2.5, the focal patterns were also calculated and shown in Fig. 6. We can see from this figure that there are two intensity peaks on optical axis for small C. Simultaneously, one dark ring also appears in geometrical focal plane, because the two on-axis intensity peaks overlap in axial direction and there is one relative weak intensity ring outside, as shown in Fig. 6**a**. On increasing C, the two intensity peaks extend in transverse direction, and the intensity ring in geometrical focal plane gets stronger at the same time. Then, those two intensity peaks

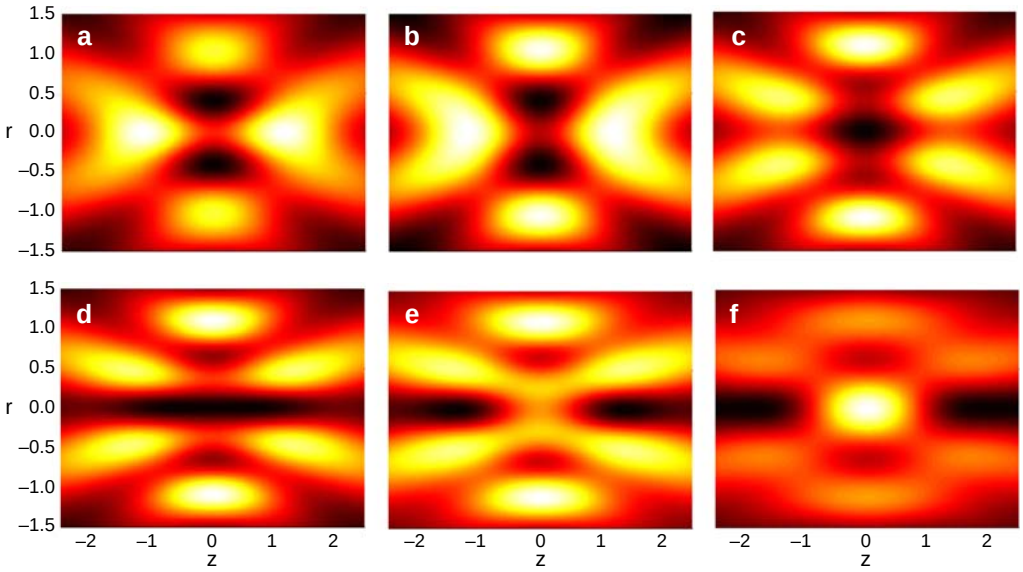

Fig. 6. Intensity distributions in focal region for NA = 0.95, β_2 = 1, β_1 = 3.5, and C = 0.0 (**a**), C = 0.2 (**b**), C = 0.4 (**c**), C = 0.6 (**d**), C = 0.8 (**e**), and C = 1.0 (**f**).

change into two intensity rings, so that there are three intensity rings in focal region, and the dark ring in geometrical focal plane shrinks to one dark focal spot, as shown in Fig. 6**c**. When parameter C continues to increase, the intensity on optical axis decreases considerably, so that dark focal spot evolves into one dark line along optical axis, as shown in Fig. 6**d**. On increasing C, the intensity at geometrical focal position increases sharply, and other intensity rings get weaker and weaker. Finally, there occurs one strong intensity peak embedded in the center of the whole focal pattern under condition of $C = 1.0$. Focal pattern may be altered remarkably by β_1 and C.

Now, the effect of parameter β_2 on focal pattern is also studied. Figure 7 illustrates the intensity distributions in focal region under condition of NA = 0.95, $\beta_2 = 2$, $\beta_1 = 0.5$, and different C. It can be seen that there is also one intensity peak for small C, and on increasing C, the center peak extends transversely, and changes into one intensity ring. By comparing Fig. 7 with Fig. 1, we can see that the focal pattern

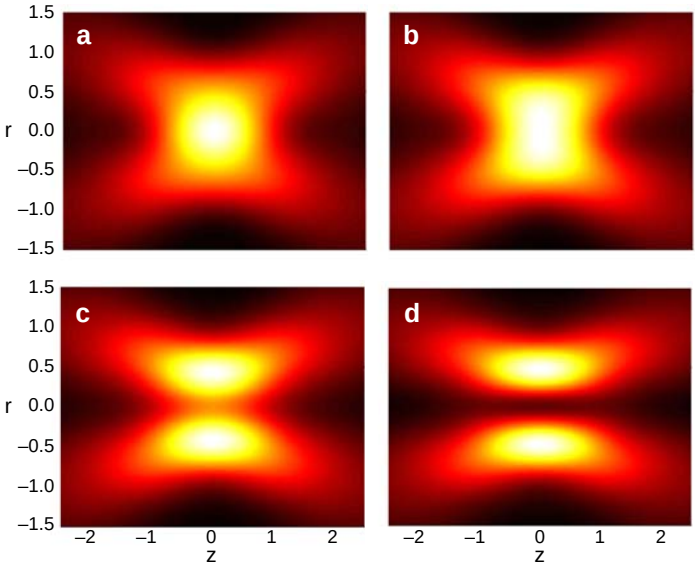

Fig. 7. Intensity distributions in focal region for NA = 0.95, $\beta_2 = 2$, $\beta_1 = 0.5$, and $C = 0.0$ (**a**), $C = 0.2$ (**b**), $C = 0.4$ (**c**), $C = 0.6$ (**d**).

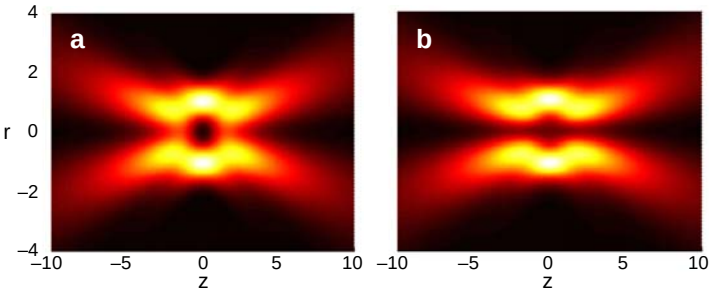

Fig. 8. Intensity distributions in focal region for NA = 0.95, $\beta_2 = 2$, $\beta_1 = 3.5$, and $C = 0.0$ (**a**), $C = 0.6$ (**b**).

evolution principle also changes for different β_2. The intensity ring does not combines back into one intensity peak for $\beta_2 = 2$, which is very different from that shown in Fig. 1. In addition, the focal patterns for $\beta_2 = 2$, $\beta_1 = 3.5$ were also calculated and shown in Fig. 8. Comparing Fig. 8 with Fig. 7, we can see one dark focal spot for $\beta_1 = 3.5$ and $C = 0.0$, while no dark focal spot occurs in Fig. 7. Under condition of higher C, intensity ring comes into being for both these cases.

For the parameter β_2 being chosen as 3, the focal patterns are shown in Fig. 9. From this figure we can see that there is one intensity ring even under condition of small C, and on increasing C, the intensity at geometrical focus point decreases continuously. Therefore, both parameters β_1 and β_2 can be used to alter the focal pattern.

The effect of numerical aperture on focal pattern was also studied. Figure 10 illustrates the focal pattern under condition of NA = 0.65, $\beta_2 = 1$, $\beta_1 = 3.5$, and

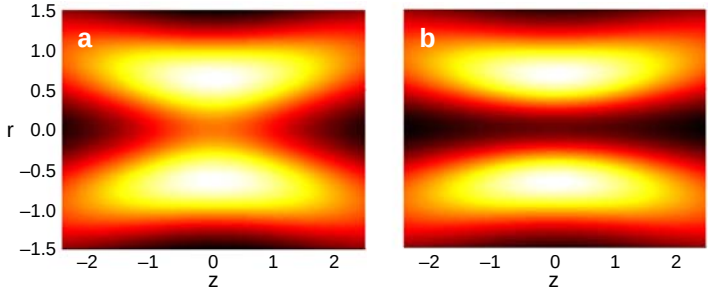

Fig. 9. Intensity distributions in focal region for NA = 0.95, $\beta_2 = 3$, $\beta_1 = 0.5$, and $C = 0.0$ (**a**), $C = 0.6$ (**b**).

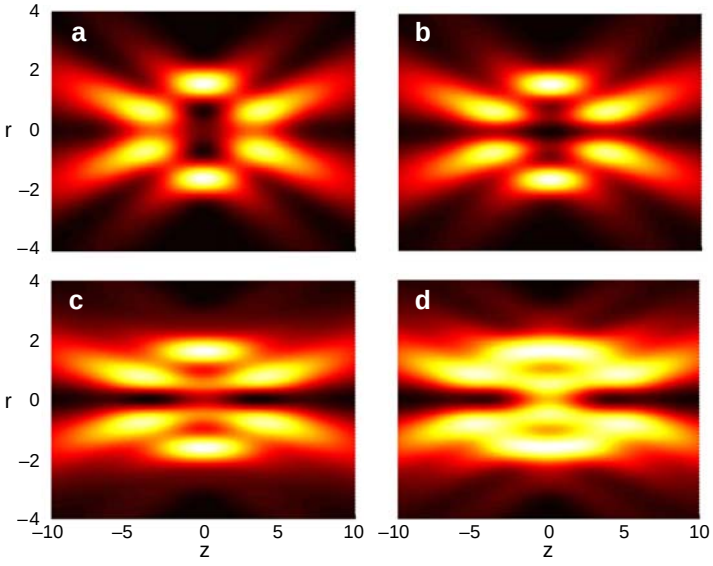

Fig. 10. Intensity distributions in focal region for NA = 0.65, $\beta_2 = 1$, $\beta_1 = 3.5$; $C = 0.0$ (**a**), $C = 0.4$ (**b**), $C = 0.8$ (**c**), $C = 1.0$ (**d**).

different C. By comparing Fig. 10 with Fig. 6, it can be seen that there is considerable focal patent difference induced by NA. For case of $C = 0.0$, the intensity maximum turns on ring shape in geometrical focal plane under NA = 0.65, while there are two intensity peaks on optical axis under NA = 0.95. And on increasing C, the whole focal pattern also changes in different principle. For instance, for the case of $C = 1.0$, there are multiple overlapping intensity rings under NA = 0.65, as shown in Fig. 10**d**, while there is only one intensity peak under NA = 0.95, as shown in Fig. 6**f**. Therefore, numerical aperture can affect focal pattern very remarkably.

4. Conclusions

We investigated the focusing properties of Bessel–Gauss beam with radial varying polarization. It was found that the intensity distribution in focal region can be altered considerably by the beam parameter and one polarization parameter that indicates the polarization change speed along radial direction. Under condition of small beam parameter, the focal spot broadens transversely, distorts into ring focus, and then evolves back into focal spot on increasing polarization angle. However, when the beam parameter increases to higher value, the whole focal pattern becomes complicated and the focus evolution principle with increasing beam parameter also changes significantly. In the focal pattern evolution process, some novel focal patterns may appear, including multiple intensity rings, dark hollow focus, cylindrical crust focus, which may be used to construct optical traps.

Acknowledgements – This work was supported by Education Commission of Zhejiang Province of China (Y200803386, Y201120426), and science and technology plan project of General Administration of Quality Supervision, Inspection and Quarantine of China (2008QK330).

References

[1] CHI K.R., *Super-resolution microscopy: Breaking the limits*, Nature Methods **6**(1), 2009, pp. 15–18.
[2] PATERSON L., MACDONALD M.P., ARLT J., SIBBETT W., BRYANT P.E., DHOLAKIA K., *Controlled rotation of optically trapped microscopic particles*, Science **292**(5518), 2001, pp. 912–914.
[3] GRIER D.G., *A revolution in optical manipulation*, Nature **424**(6950), 2003, pp. 810–816.
[4] MACDONALD M.P., SPALDING G.C., DHOLAKIA K., *Microfluidic sorting in an optical lattice*, Nature **426**(6965), 2003, pp. 421–424.
[5] XIUMIN GAO, FUXI GAN, WENDONG XU, *Superresolution by three-zone pure phase plate with 0, π, 0 phase variation*, Optics and Laser Technology **39**(5), 2007, pp. 1074–1080.
[6] RITTWEGER E., KYU YOUNG HAN, IRVINE S.E., EGGELING C., HELL S.W., *STED microscopy reveals crystal colour centres with nanometric resolution*, Nature Photonics **3**(3), 2009, pp. 144–147.
[7] VISSCHER K., BRAKENHOFF G.J., *Theoretical study of optically induced forces on spherical particles in a single beam trap I: Rayleigh scatterers*, Optik **89**, 1992, pp. 174–180.
[8] XIUMIN GAO, ZHOU FEI, WENDONG XU, FUXI GAN, *Focus splitting induced by a pure phase-shifting apodizer*, Optics Communications **239**(1–3), 2004, pp. 55–59.
[9] ARLT J., PADGETT M.J., *Generation of a beam with a dark focus surrounded by regions of higher intensity: The optical bottle beam*, Optics Letters **25**(4), 2000, pp. 191–193.

[10] GBUR G., VISSER T.D., *Can spatial coherence effects produce a local minimum of intensity at focus?*, Optics Letters **28**(18), 2003, pp. 1627–1629.
[11] GANIC D., XIAOSONG GAN, MIN GU, HAIN M., SOMALINGAM S., STANKOVIC S., TSCHUDI T., *Generation of doughnut laser beams by use of a liquid-crystal cell with a conversion efficiency near 100%*, Optics Letters **27**(15), 2002, pp. 1351–1353.
[12] QIWEN ZHAN, *Cylindrical vector beams: from mathematical concepts to applications*, Advances in Optics and Photonics **1**(1), 2009, pp. 1–57.
[13] QIWEN ZHAN, LEGER J.R., *Focus shaping using cylindrical vector beams*, Optics Express **10**(7), 2002, pp. 324–330.
[14] YOUNGWORTH K.S., BROWN T.G., *Focusing of high numerical aperture cylindrical-vector beams*, Optics Express **7**(2), 2000, pp. 77–87.
[15] XIUMIN GAO, MINGYU GAO, SONG HU, HANMING GUO, JIAN WANG, SONGLIN ZHUANG, *High focusing of radially polarized Bessel-modulated Gaussian beam*, Optica Applicata **40**(4), 2010, pp. 965–974.
[16] XIUMIN GAO, QIUFANG ZHAN, JINSONG LI, SONG HU, JIAN WANG, SONGLIN ZHUANG, *Cylindrical vector axisymmetric Bessel-modulated Gaussian beam*, Optical and Quantum Electronics **41**(5), 2009, pp. 385–396.
[17] ORON R., BLIT S., DAVIDSON N., FRIESEM A.A., BOMZON Z., HASMAN E., *The formation of laser beams with pure azimuthal or radial polarization*, Applied Physics Letters **77**(21), 2000, pp. 3322–3324.
[18] HAIFENG WANG, LUPING SHI, LUKYANCHUK B., SHEPPARD C., CHONG TOW CHONG, *Creation of a needle of longitudinally polarized light in vacuum using binary optics*, Nature Photonics **2**(8), 2008, pp. 501–505.
[19] YAJUN LI, GUREVICH V., KIRCHEVER M., KATZ J., MAROM E., *Propagation of anistropic Bessel––Gaussian beams: Sidelobe control, mode selection, and field depth*, Applied Optics **40**(16), 2001, pp. 2709–2721.
[20] YUANJIE YANG, YUDE LI, *Spectral shifts and spectral switches of a pulsed Bessel–Gauss beam from a circular aperture in the far field*, Optics and Laser Technology **39**(8), 2007, pp. 1478–1484.
[21] EYYUBOGLU H.T., HARDALAC F., *Propagation of modified Bessel–Gaussian beams in turbulence*, Optics and Laser Technology **40**(2), 2008, pp. 343–351.
[22] ORLOV S., STABINIS A., *Free-space propagation of light field created by Bessel–Gauss and Laguerre–Gauss singular beams*, Optics Communications **226**(1–6), 2003, pp. 97–105.
[23] XIAOLING JI, BAIDA LÜ, *Focal shift and focal switch of Bessel–Gaussian beams passing through a lens system with or without aperture*, Optics and Laser Technology **39**(3), 2007, pp. 562–568.
[24] YUAN G.H., WEI S.B., YUAN X.-C., *Nondiffracting transversally polarized beam*, Optics Letters **36**(17), 2011, pp. 3479–3481.
[25] LITVIN I.A., FORBES A., *Bessel–Gauss resonator with internal amplitude filter*, Optics Communications **281**(9), 2008, pp. 2385–2392.
[26] XIU-MIN GAO, SONG HU, JIN-SONG LI, ZUO-HONG DING, HAN-MING GUO, SONG-LIN ZHUANG, *Tunable optical gradient trap by radial varying polarization Bessel–Gauss beam*, Journal of Biomedical Science and Engineering **3**(3), 2010, pp. 304–307.
[27] YEW E.Y.S., SHEPPARD C.J.R., *Tight focusing of radially polarized Gaussian and Bessel–Gauss beams*, Optics Letters **32**(23), 2007, pp. 3417–3419.

Received November 17, 2011
in revised form December 23, 2011